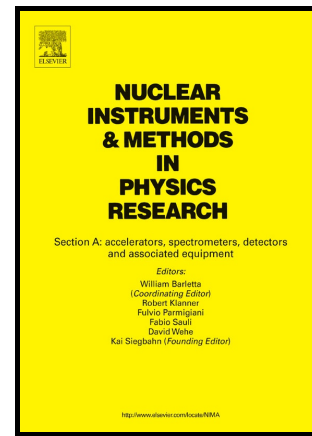


Author's Accepted Manuscript

Test of Ultra Fast Silicon Detectors for Picosecond Time Measurements with a New Multipurpose Read-Out Board

N. Minafra, H. Al Ghouf, R. Arcidiacono, N. Cartiglia, L. Forthomme, R. Mulargia, M. Obertino, C. Royon



www.elsevier.com/locate/nima

PII: S0168-9002(17)30482-5
DOI: <http://dx.doi.org/10.1016/j.nima.2017.04.032>
Reference: NIMA59820

To appear in: *Nuclear Inst. and Methods in Physics Research, A*

Received date: 11 March 2017
Revised date: 17 April 2017
Accepted date: 19 April 2017

Cite this article as: N. Minafra, H. Al Ghouf, R. Arcidiacono, N. Cartiglia, L. Forthomme, R. Mulargia, M. Obertino and C. Royon, Test of Ultra Fast Silicon Detectors for Picosecond Time Measurements with a New Multipurpose Read Out Board, *Nuclear Inst. and Methods in Physics Research, A* <http://dx.doi.org/10.1016/j.nima.2017.04.032>

This is a PDF file of an unedited manuscript that has been accepted for publication. As a service to our customers we are providing this early version of the manuscript. The manuscript will undergo copyediting, typesetting, and review of the resulting galley proof before it is published in its final citable form. Please note that during the production process errors may be discovered which could affect the content, and all legal disclaimers that apply to the journal pertain

1 Test of Ultra Fast Silicon Detectors for Picosecond
2 Time Measurements with a New Multipurpose
3 Read-Out Board

4 N. Minafra^a, H. Al Ghoula^a, R. Arcidiacono^d, N. Cartiglia^b, L. Forthomme^a,
5 R. Mulargia^{b,c}, M. Obertino^c, C. Royon^a

6 ^a*University of Kansas, Lawrence, USA.*

7 ^b*INFN, Torino, Italy.*

8 ^c*Università di Torino, Torino, Italia and INFN, Torino, Italy*

9 ^d*Università del Piemonte Orientale, Italia and INFN, Torino, Italy*

10 **Abstract**

Ultra Fast Silicon Detectors (UFSD) are sensors optimized for timing measurements employing a thin multiplication layer to increase the output signal. A multipurpose read-out board hosting a low-cost, low-power fast amplifier was designed at the University of Kansas and tested at the European Organization for Nuclear Research (CERN) using a 180 GeV pion beam. The amplifier has been designed to read out a wide range of detectors and it was optimized in this test for the UFSD output signal. In this paper we report the results of the experimental tests using 50 μm thick UFSD with a sensitive area of 1.4 mm². A timing precision below 30 ps was achieved.

11 *Keywords:* Time-of-flight, Time precision, Ultra Fast Silicon Detectors,
12 Charge Sensitive Amplifier, Picosecond Time Measurement

13 **1. Introduction**

14 The increasing demand for better timing and spatial resolution has been the
15 key purpose for developing new type of sensors. Low Gain Avalanche Detector
16 (LGAD) technology is one of the most promising advancements in silicon detector
17 technology as it allows a sensible increase of the detector output signal,
18 while keeping all of the known advantages of a silicon substrate, such as low
19 cost and large scale production capabilities. A sensor with an enhanced output

Email address: nicola.minafra@cern.ch (N. Minafra)

20 signal can also be used for tracking since a large signal simplifies the design of
21 the front-end electronics; however, its most innovative application is for precise
22 timing. When a particle detector is crossed by a minimum ionizing particle
23 (MIP), free charge carriers are produced inside the sensitive region. An output
24 signal is then produced when these charge carriers start drifting towards the
25 electrodes where they will be collected. The duration of the signal depends on
26 the length of the collection process; therefore a thin sensor produces a faster
27 signal. On the other hand, a thin sensor has a small sensitive volume and,
28 therefore, produces a smaller signal. With the LGAD technology it is possible
29 to create a thin sensor that produces a signal 10 to 20 times larger than the
30 equivalent traditional sensor. Thin LGAD sensors optimized for precise time
31 measurements, also known as UFSD, have been developed by CNM [1].

32 A multipurpose read-out board has been developed to test different type
33 of sensors and it has been optimized in this test for the UFSD characteristics.
34 This board can be used to perform a full characterization of the sensor, i.e.
35 current/voltage (IV) characteristics, capacitance measurement, test with pulsed
36 lasers, radioactive sources and particle beams.

37 In section 2 the multipurpose read-out board will be described, with partic-
38 ular focus on the optimization of the parameters of the amplifier to $50\ \mu\text{m}$ thick
39 UFSD. The following section describes how the board was used to characterize
40 the sensor in the North Area at CERN. Finally, in section 4, the results are
41 presented and discussed.

42 **2. The multipurpose read-out board**

43 In this section, the multipurpose read-out board will be described: first the
44 layout of the board is discussed, then the optimization process for a particular
45 detector, using numerical simulations, is illustrated.

46 The read-out board has been designed to host solid state sensors of differ-
47 ent types such as UFSD, traditional silicon detectors, Silicon PhotoMultipliers
48 (SiPMs) as well as diamond detectors. The board includes an amplifier that can

49 be configured to have a very large bandwidth, for instance when reading SiPMs
 50 or high gain Avalanche PhotoDiodes (APDs), or to optimize the signal-to-noise
 51 ratio (SNR) when reading diamond detectors and LGADs.

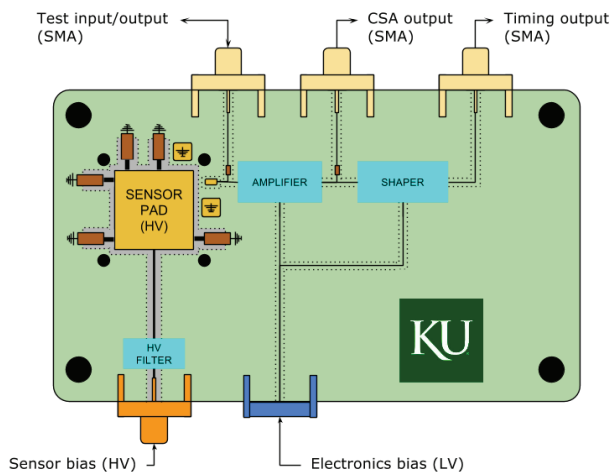


Figure 1: Layout of the front-end board. Different connectors are used for the sensor, electronics bias, signal inputs and outputs.

52 The board can distribute a bias potential up to 1 kV through a 20x20 mm²
 53 pad on which the sensor is glued. Grounded pads are also available to connect
 54 a sensor's guard ring. Finally, the amplifier is DC-coupled to the sensor. The
 55 test board allows reading out the signal at various stages, as shown in Fig. 1:

- 56 • directly from the sensor;
- 57 • after a low noise charge sensitive amplifier (CSA);
- 58 • after a shaping stage optimized for time measurements.

59 The first connector can also be used to send a calibration signal to the amplifier.

60 One of the main contributions to the time precision of a detector is the jitter,
 61 which can be approximated to¹:

¹An extended discussion of the different contributions that affect a time measurements is done in chapter 6 of [2].

$$\sigma_t \approx \sigma_{noise} \cdot \frac{\tau}{A} = \frac{\tau}{SNR} = 1.25 \frac{\tau_{0.1-0.9}}{SNR}, \quad (1)$$

62 where τ is the rise time of the signal, $\tau_{0.1-0.9}$ is the 10% to 90% rise time; A
 63 is the amplitude and σ_{noise} is the RMS of the noise. In this approximation, a
 64 large SNR with a slow signal or a small SNR with a fast signal are equivalent.

65 The electronics can be optimized for different sensors using numerical sim-
 66 ulations, starting from a model of the sensor. In particular, it is possible to
 67 increase or decrease the gain of the last stage of amplification (with a negligible
 68 effect on the SNR) or to change the time constant of the shaper: a larger time
 69 constant is needed to produce a slower signal with improved SNR.

70 In this work, the amplifier parameters were optimized for 50 μm UFSDs, for
 71 MIP detection and for a signal read-out using a fast sampling device, like an
 72 oscilloscope or the SAMPIC chip [3]. Thanks to the large signal produced by
 73 the sensor, the time constant of the amplifier was reduced below 1 ns, enough to
 74 have a good SNR. Then, the final stage was tuned to produce a signal amplitude
 75 (for the MIP) around 100 mV, to cope with the dynamic range of the SAMPIC
 76 chip.

77 The equivalent model of the sensor used to simulate the electronics is a
 78 current generator, in parallel with a capacitor and a resistor. This resistor can
 79 be neglected if the dark current is low, as shown in Fig. 2. It is also possible to
 80 include the parasitic effects of the input connection, i.e. bonding wire, bonding
 81 pad, and path to the amplifier among others. The dominant effects are due
 82 to the capacitance of the sensor and to the inductance and resistance of the
 83 bonding wire.

84 The current produced by the detector was simulated using `Weightfield2` [4]
 85 and an analytic replica was used as input to the amplifier simulation. This ap-
 86 proach works for all sensors simulated by the software, i.e. silicon and diamond
 87 detectors and UFSD of any given thickness and geometry.

88 Fig. 3 shows the expected output amplitude for a 50 μm UFSD. The gain for
 89 low input charge is $\approx 7 \text{ mV/fC}$, while the expected noise RMS is $\approx 0.23 \text{ fC} \approx$

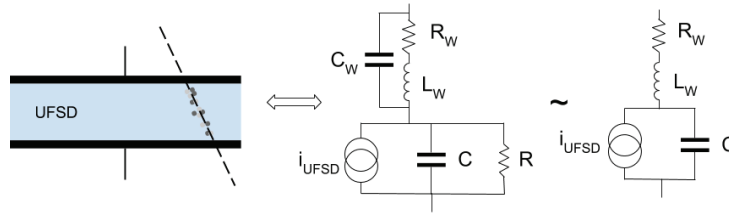


Figure 2: Sketch of the sensor equivalent circuit. The sensor can be simulated as a current generator in parallel with a capacitor and connected to the amplifier through an inductor and a resistor.

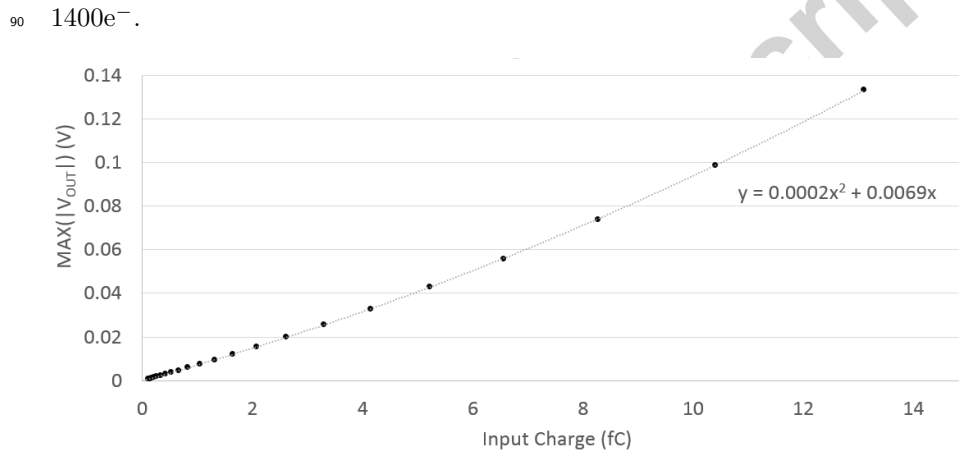


Figure 3: The simulated output of the amplifier connected to a $50 \mu\text{m}$ UFSD can be assumed linear for small input charges ($< 4 \text{ fC}$), equal to $\approx 7 \text{ mV/fC}$ while for higher values a parabola is needed.

91 The simulation of the electronics also gives suggestions on the parameters
 92 to be used to minimize the jitter. For example, using a constant fraction dis-
 93 criminators the best performance is obtained using a threshold at 50% of the
 94 amplitude, as the derivative of the signal is maximum at that point as shown in
 95 Fig. 4.

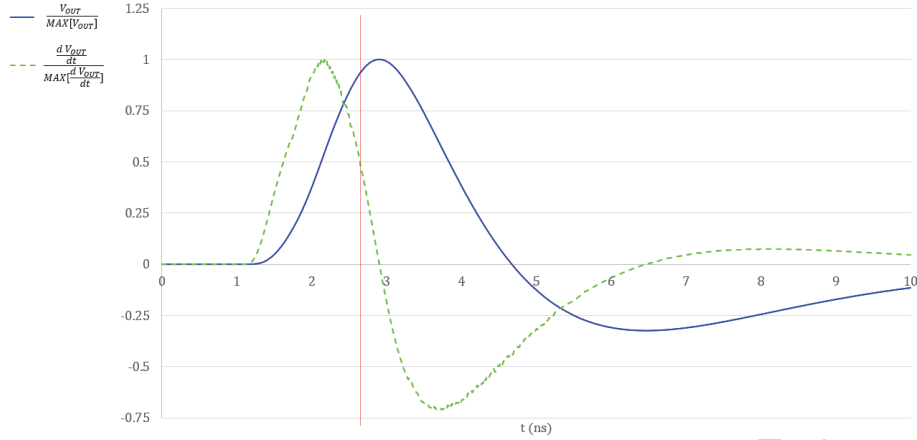


Figure 4: The signal slope is maximum at 50% of the maximum amplitude.

96 3. Test on particle beam

97 The board, i.e. Device Under Test (DUT), was installed on a test bench at
 98 CERN in the H8 experimental area on an SPS secondary beam. In this section,
 99 the test setup will be described.

100 The signal was read using an oscilloscope (*Agilent DSO9254A*) acquiring at
 101 20 GS/s. The time precision was measured using as a reference a 10 mm long
 102 quartz bar of 9 mm² glued on a *SensL* Silicon Photomultiplier (SiPM) of the
 103 same surface, installed on an evaluation board of the same manufacturer [5].

104 An additional detector, a quartz bar installed on a MCP-PMT *Planacon*
 105 XP85012, was used to cross check the measurement of the time precision. By
 106 measuring the time difference between each combination of two detectors, it is
 107 possible to uniquely compute their time precision, using the setup shown in Fig.
 108 5:

$$\begin{cases} \sigma_{DUT}^2 + \sigma_{SiPM}^2 = \sigma_{SiPM-DUT}^2 \\ \sigma_{SiPM}^2 + \sigma_{MCP}^2 = \sigma_{MCP-SiPM}^2 \\ \sigma_{MCP}^2 + \sigma_{DUT}^2 = \sigma_{MCP-DUT}^2, \end{cases} \quad (2)$$

where σ_{DUT} is the time precision of the DUT, σ_{SiPM} is the time precision of

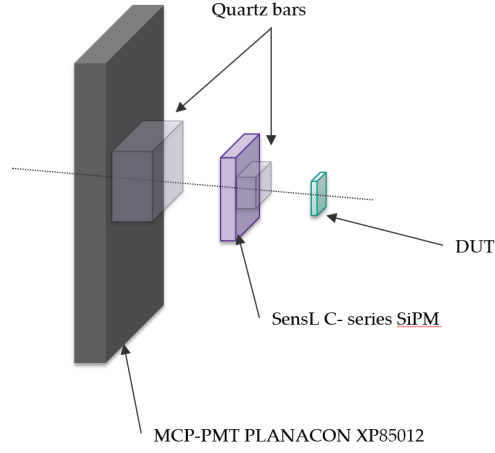


Figure 5: Schematic of the experimental setup. A SiPM was used as time reference and a MCP-PMT was used to measure the time precision of the SiPM.

the SiPM and σ_{MCP} is the time precision of the MCP-PMT; while σ_{i-j} are the standard deviation of the measured time difference between device i and j . Hence the individual time precisions are given by

$$\begin{cases} \sigma_{DUT}^2 = (\sigma_{SiPM-DUT}^2 - \sigma_{MCP-SiPM}^2 + \sigma_{MCP-DUT}^2)/2 \\ \sigma_{SiPM}^2 = (\sigma_{MCP-SiPM}^2 - \sigma_{MCP-DUT}^2 + \sigma_{SiPM-DUT}^2)/2 \\ \sigma_{MCP}^2 = (\sigma_{MCP-DUT}^2 - \sigma_{SiPM-DUT}^2 + \sigma_{MCP-SiPM}^2)/2 \end{cases} \quad (3)$$

109 Using these equations, the time precision of the SiPM was estimated to be
 110 ≈ 18 ps and the precision of the MCP-PMT ≈ 22 ps. The error on these
 111 measurements was estimated to be of the order of 5%.

112 The alignment of the detectors was insured by a mechanical structure, shown
 113 in Fig. 6.

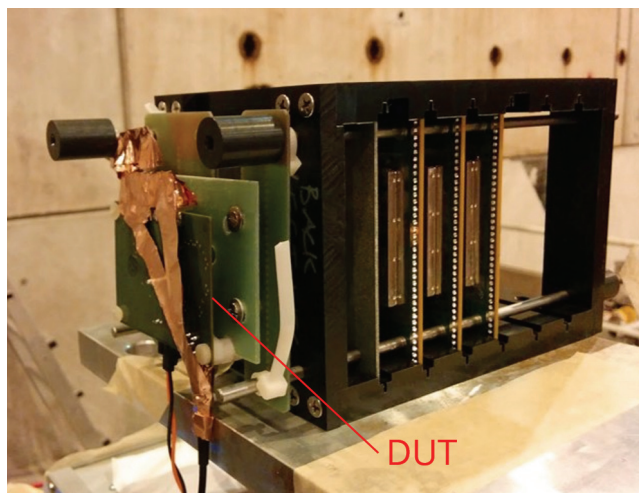


Figure 6: Picture of the experimental setup. The DUT is installed on a support structure to ease the alignment.

114 4. Beam test results

115 Data acquired during the beam test have been analyzed and the results will
 116 be presented and discussed in this section.

117 One may investigate the performance of the sensor at different gain values.
 118 The latter can be controlled by increasing the bias voltage [6]. The amplitude
 119 of the output signal depends, for a fixed gain, on the charge deposited by the
 120 passage of the particle; therefore, the distribution of the signal amplitude should
 121 follow a Landau distribution. However, if noise is added to the signal, the
 122 amplitude will be distributed as a Landau convoluted with a Gaussian. The
 123 parameters of the Landau distribution are the most probable value (MPV) and
 124 the width, that is 1/4 of the Full Width Half Maximum (FWHM); the σ of the
 125 Gaussian ($G\text{Sigma}$) is an estimation of noise and fluctuations. This convolution
 126 fits the data very well as it can be seen in Fig. 7, showing the amplitude
 127 distribution at a bias voltage of 180 V.

128 The MPV depends on the gain, hence the bias voltage, while the amplifier
 129 noise is independent from the latter. The SNR has the same dependence of the
 130 MPV, as shown in Fig. 8.

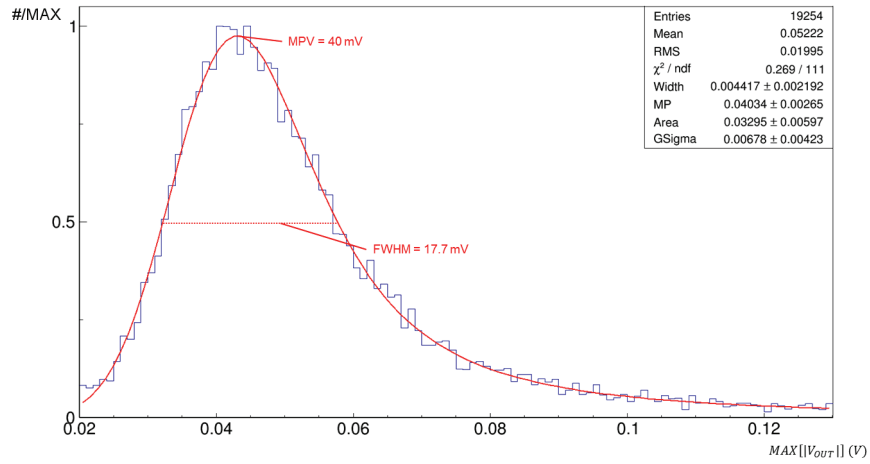


Figure 7: Amplitude of the amplified signal produced by the UFSD biased at 180 V. The distribution obtained convolving a Landau with a Gaussian that best fits the data and its parameters are also shown.

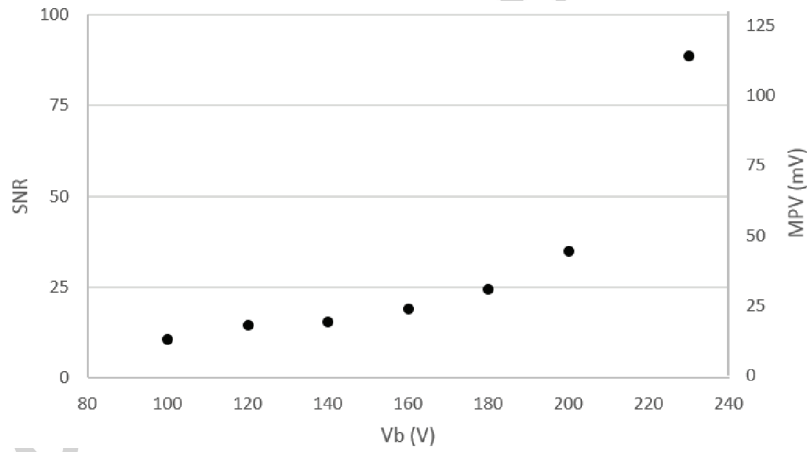


Figure 8: Dependence of the measured signal amplitude (Most Probable value) and of the SNR increasing the biasing voltage V_b , computed considering only the noise contribution of the amplifier that is constant $\sigma_v \approx 1.5$ mV.

131 The term $GSigma$ has two main contributions, from the sensor, i.e. shot
 132 noise, and from the amplifier: $GSigma^2 \approx \sigma_{sensor}^2 + \sigma_{amplifier}^2$. The contribution
 133 of the amplifier can be measured in absence of particles (fluctuation of the
 134 pedestal). It was measured to be constant even among different acquisitions

135 taken with different environmental factors (temperature, radiofrequency pick-
 136 ups, etc).

137 The behaviour of the ratio between the MPV and the Full Width at Half
 138 of the Maximum (FWHM) of the amplitude distribution² was investigated. As
 139 shown in Fig. 9, this ratio mainly depends on the thickness of the sensor and
 140 the value is expected to be around 0.6 for a 50 μm thick silicon sensor [7].

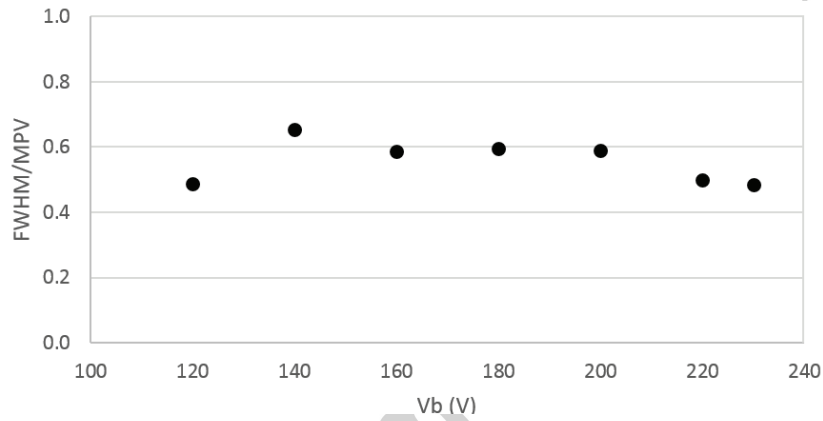


Figure 9: The stochastic behaviour of the signal amplitude can be described by the Landau distribution. The ratio between the Full Width at Half of the Maximum and the Most Probable Value of this distribution is expected to be close to 0.6 for a 50 μm thick silicon sensor [7].

141 The gain of the sensor is investigated measuring the amplitude of the signal
 142 for different bias voltages, normalized to the simulated amplitude for an equiv-
 143 alent sensor without the gain layer (gain = 1). The results are shown in Fig. 10
 144 and are in good agreement with the results found in other works, for example
 145 [8]. Fig. 11 shows that the noise $GSigma$ increases linearly with the gain.

146 Finally, using a SiPM as time reference (see section 3), the precision of the
 147 measured time of arrival was computed for different settings, using an off-line
 148 Constant Fraction Discriminator (CFD). The dependency on the fraction used
 149 in the CFD (k_{CFD}) is shown in Fig. 12 for various bias voltages. As discussed

²These values are computed directly from the histogram of the amplitude, without using a Landau distribution, i.e. without deconvolving the noise.

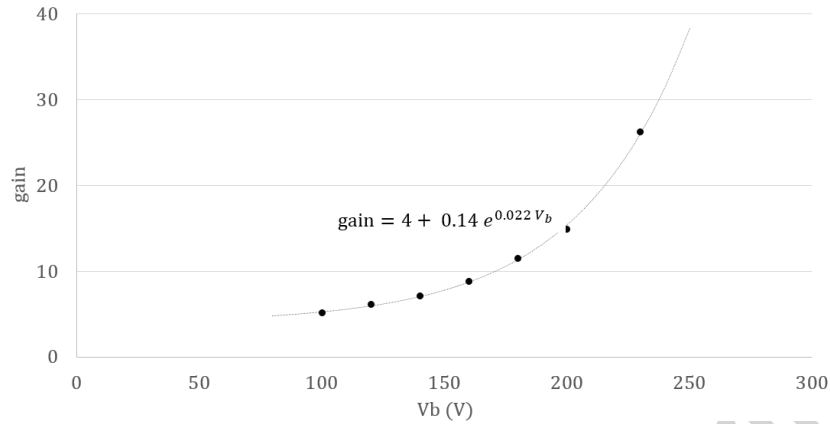


Figure 10: Dependence of the gain of the UFSD on the applied biasing voltage. The black dots represent the measured values and the equation of the exponential function that best fits the data is also shown.

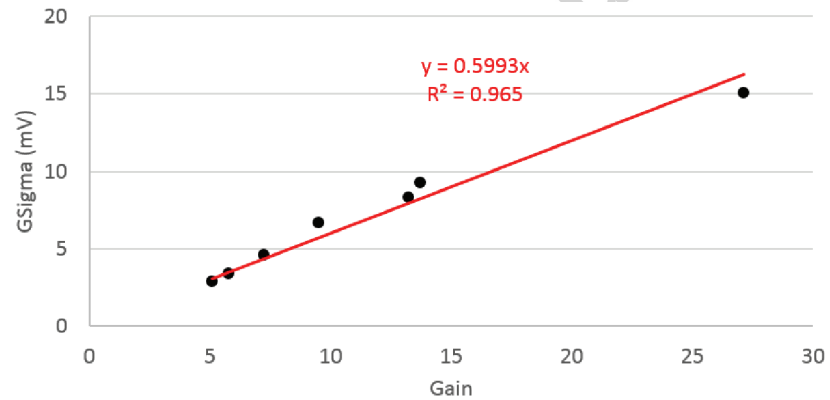


Figure 11: The parameter $GSigma$ is an indication of the noise produced by the sensor and increases linearly with gain. The red solid line is a linear interpolation obtained requiring $GSigma = 0$ with no gain.

150 in section 2, the best ratio to minimize the jitter is around 50%, while for higher
 151 gain, where the jitter is negligible, a lower value is preferable.

152 As shown in Fig. 13, the time precision is improved increasing the bias
 153 voltage. A deviation from the precision expected using eq. 1 is noticeable and
 154 the deviation can be attributed to the non linear rising edge of the signal and
 155 to the Landau noise [9].

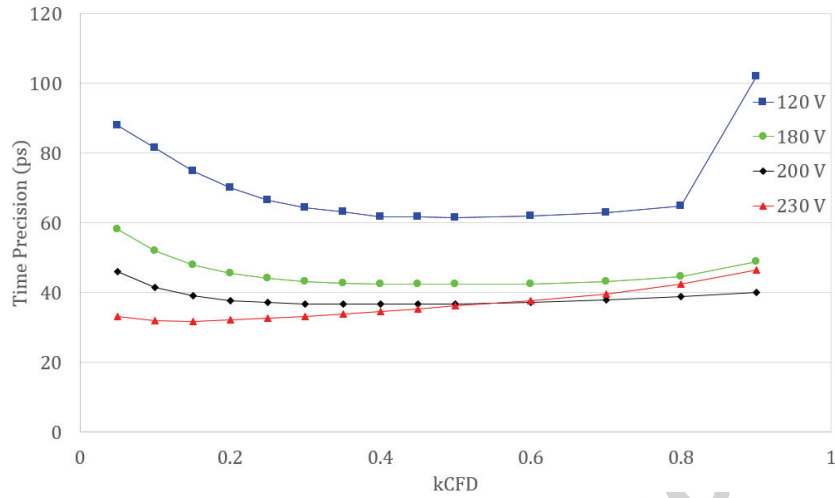


Figure 12: Dependence of the measured time precision on the fraction used for the CFD. The best CFD ratio is 0.5, as expected from simulations; however, when the biasing voltage is high, i.e. high gain, the behaviour is different.

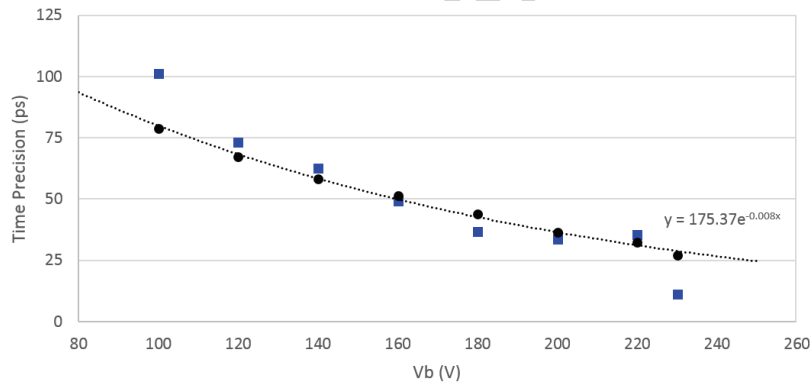


Figure 13: Dependence of the measured time precision on the biasing voltage. The black circles are the measured values using the best value of k_{CFD} , while the blue squares are the time precision computed using eq. 1 considering only the noise of the amplifier.

156 Fig. 14 shows the difference between the time of arrival measured using the
 157 UFSD under test and the time reference.

158 The data presented in this section indicate that the multipurpose board is an
 159 excellent tool for the characterization of solid state sensors and, in combination
 160 with the latest generation of UFSD, can reach a time precision below 30 ps for

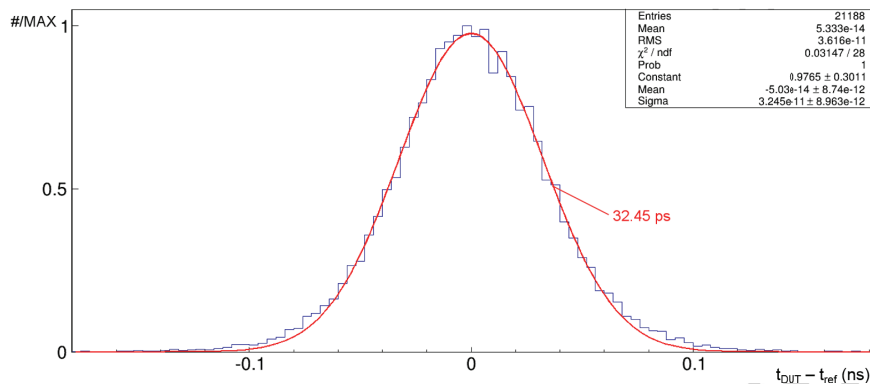


Figure 14: Time difference between the UFSD under test, biased at 230 V, and the time reference, time precision of the UFSD is $\approx \sqrt{\sigma^2 - \sigma_{ref}^2} \approx 27$ ps

161 MIPs.

162 5. Conclusion

163 The design, realization, and test of a general purpose front-end board for
 164 solid state detectors was discussed in this work. The board was specifically
 165 designed for precise time measurements using a sampling device, such as a digital
 166 oscilloscope or a SAMPIC chip. It was tested using a 50 μm thick UFSD and
 167 a time precision down to 27 ps was measured with a pion beam in the North
 168 Area at CERN. A more compact and low power version of the amplifier is
 169 under development and is specifically designed for applications where compact
 170 electronics are needed but the development of a dedicated integrated circuit is
 171 not feasible for time nor cost constraints.

172 6. Acknowledgements

173 The authors would like to thank the TOTEM Collaboration for generously
 174 giving up part of their beam time in the North Area at CERN to allow per-
 175 forming the tests discussed in this paper and also the RD50 Collaboration for
 176 the sensors production and UCSC for the time reference.

177 The work was supported by the United States Department of Energy, grant
178 DE-FG02-04ER41286. Part of this work has been financed by the Spanish Min-
179 istry of Economy and Competitiveness through the Particle Physics National
180 Program (FPA2015-69260-C3-3-R and FPA2014-55295-C3-2-R), by the Euro-
181 pean Union's Horizon 2020 Research and Innovation funding program, under
182 Grant Agreement no. 654168 (AIDA-2020) and Grant Agreement no. 669529
183 (ERC UFSD669529), and by the Italian Ministero degli Affari Esteri and INFN
184 Gruppo V.

185 References

- 186 [1] G. Pellegrini et al. Technology developments and first measurements of Low
187 Gain Avalanche Detectors (LGAD) for high energy physics applications. *Nu-*
188 *clear Instruments and Methods in Physics Research Section A: Accelerators,*
189 *Spectrometers, Detectors and Associated Equipment*, 765:12 – 16, 2014.
- 190 [2] N. Minafra. *Development of a timing detector for the TOTEM experiment at*
191 *the LHC*. PhD thesis, Bari, University of Bari A. Moro, Feb 2016. Presented
192 14 Mar 2016.
- 193 [3] D. Breton, V. De Cacqueray, E. Delagnes, H. Grabas, J. Maalmi, N. Minafra,
194 C. Royon, and M. Saimpert. Measurements of timing resolution of ultra-fast
195 silicon detectors with the SAMPIC waveform digitizer. *Nuclear Instruments*
196 *and Methods in Physics Research Section A: Accelerators, Spectrometers,*
197 *Detectors and Associated Equipment*, 835:51 – 60, 2016.
- 198 [4] F. Cenna, N. Cartiglia, M. Friedl, B. Kolbinger, H. F.-W. Sadrozinski, A. Sei-
199 den, A. Zatserklyaniy, and A. Zatserklyaniy. Weightfield2: A fast simulator
200 for silicon and diamond solid state detector. *Nuclear Instruments and Meth-*
201 *ods in Physics Research Section A: Accelerators, Spectrometers, Detectors*
202 *and Associated Equipment*, 2015.
- 203 [5] Low Noise, Blue-Sensitive Silicon Photomultipliers. [http://sens1.com/](http://sens1.com/downloads/ds/DS-MicroCseries.pdf)
204 [downloads/ds/DS-MicroCseries.pdf](http://sens1.com/downloads/ds/DS-MicroCseries.pdf).

- 205 [6] H. F.-W. Sadrozinski, M. Baselga, S. Ely, V. Fadeyev, Z. Galloway, J. Ngo,
206 C. Parker, D. Schumacher, A. Seiden, A. Zatserklyaniy, et al. Sensors for
207 ultra-fast silicon detectors. *Nuclear Instruments and Methods in Physics*
208 *Research Section A: Accelerators, Spectrometers, Detectors and Associated*
209 *Equipment*, 765:7–11, 2014.
- 210 [7] S. Meroli, D. Passeri, and L. Servoli. Energy loss measurement for
211 charged particles in very thin silicon layers. *Journal of Instrumentation*,
212 6(06):P06013, 2011.
- 213 [8] N. Cartiglia et al. Beam test results of a 15 ps timing system based on
214 ultra-fast silicon detectors. *arXiv preprint arXiv:1608.08681*, 2016.
- 215 [9] N. Cartiglia et al. Tracking in 4 dimensions. *Nuclear Instruments and Meth-*
216 *ods in Physics Research Section A: Accelerators, Spectrometers, Detectors*
217 *and Associated Equipment*, 845:47 – 51, 2017. Proceedings of the Vienna
218 Conference on Instrumentation 2016.